ACS Catalysis

Letter

Cite This: ACS Catal. 2018, 8, 8314–8317

pubs.acs.org/acscatalysis

Regioselectivity Engineering of Epoxide Hydrolase: Near-Perfect Enantioconvergence through a Single Site Mutation

Fu-Long Li,[†,#] Xu-Dong Kong,[†,‡,#] Qi Chen,[†] Yu-Cong Zheng,[†] Qin Xu,[§] Fei-Fei Chen,[†] Li-Qiang Fan,[†] Guo-Qiang Lin,[‡] Jiahai Zhou,[*,‡] Hui-Lei Yu,[*,†] and Jian-He Xu[*,†]

[†]State Key Laboratory of Bioreactor Engineering, Shanghai Collaborative Innovation Center for Biomanufacturing Technology, East China University of Science and Technology, Shanghai 200237, China

[‡]Center for Excellence in Molecular Synthesis, Shanghai Institute of Organic Chemistry, Chinese Academy of Sciences, Shanghai 200032, China

[§]State Key Laboratory of Microbial Metabolism, and School of Life Sciences and Biotechnology, Shanghai Jiao Tong University, Shanghai 200240, China

Supporting Information

ABSTRACT: An epoxide hydrolase from *Vigna radiata* (*Vr*EH2) affords partial enantioconvergence (84% *ee*) in the enzymatic hydrolysis of racemic *p*-nitrostyrene oxide (pNSO), mainly due to insufficient regioselectivity for the (*S*)-enantiomer ($r_S = \alpha_S/\beta_S = 7.3$). To improve the (*S*)-pNSO regioselectivity, a small but smart library of *Vr*EH2 mutants was constructed by substituting each of four key residues lining the substrate binding site with a simplified amino acid alphabet of Val, Asn, Phe, and Trp. Among the mutants, M263N attacked almost exclusively at Cα in the (*S*)-epoxide ring with satisfactory regioselectivity (r_S = 99.0), without compromising the original high regioselectivity for the (*R*)-epoxide (r_R = 99.0), resulting in near-perfect enantioconvergence (>99% analytical yield, 98% *ee*). Structural and conformational analysis showed that the introduced Asn263 formed additional hydrogen bonds with the nitro group in substrate, causing a shift in the substrate binding pose. This shift increased the difference in attacking distances between Cα and Cβ, leading to an improved regiopreference toward (*S*)-pNSO and affording near-perfect enantioconvergence.

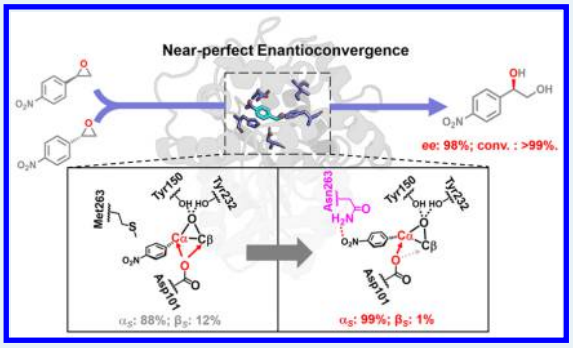

KEYWORDS: *biocatalysis, epoxide hydrolase, crystal structure, regioselectivity, enantioconvergence, protein engineering*

Optically pure epoxides and vicinal diols are important building blocks for the preparation of chiral drugs and bioactive compounds, such as adrenergic inhibitors and antiobesity drugs.[1] The hydrolysis of racemic epoxides by epoxide hydrolases (EHs; EC 3.3.2.3) is often reported as a green route to accessing enantiopure epoxides or vicinal diols.[2] However, the majority of EH-catalyzed classical kinetic resolutions of racemic epoxides are disadvantageous due to the maximum yield being limited to 50%.[3] As an alternative pathway, enantioconvergent processes (Scheme 1) catalyze the hydrolysis of two opposite enantiomers of an epoxide with complementary regioselectivity,[4] in which Cα of the epoxide ring is preferentially attacked in one enantiomer, giving the product with an inverted configuration, while Cβ is preferentially attacked in the other enantiomer affording the diol in a retained configuration. Overall, the enantioenriched diol can be produced with a maximum theoretical yield of 100%.[5]

Since the first reports of enantioconvergence using EHs by the groups of Faber and Furstoss,[6] EH-mediated enantioconvergent hydrolysis has attracted much attention. Nonetheless, studies on EH-mediated enantioconvergent hydrolysis are still hampered by the insufficient degree of enantioconvergence afforded by previously reported native EHs (Table S1).[6b,7] In our previous work, *Vr*EH2, one of the two epoxide hydrolases cloned from *Vigna radiata* showed a partial degree of enantioconvergence

Scheme 1. Overview of the EH-Catalyzed Enantioconvergent Hydrolysis of Epoxides[a]

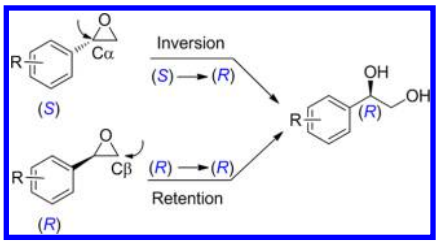

[a]Cα of epoxide ring in one enantiomer (in this case (*S*)-epoxide) is preferentially attacked, giving (*R*)-diol with an inverted configuration, while Cβ of (*R*)-epoxide is preferentially attacked, giving the diol with a retained configuration (*R*).

Received: July 6, 2018
Revised: August 3, 2018
Published: August 8, 2018

Downloaded via SHANGHAI JIAO TONG UNIV on November 21, 2018 at 02:36:27 (UTC).
See https://pubs.acs.org/sharingguidelines for options on how to legitimately share published articles.

© 2018 American Chemical Society

DOI: 10.1021/acscatal.8b02622
ACS Catal. 2018, 8, 8314–8317

(only 84% *ee*) in the enzymatic hydrolysis of racemic *p*-nitrostyrene oxide (*rac*-pNSO). This was mainly attributed to the low regioselectivity toward (*S*)-pNSO (attacking ratio of alpha carbon (Cα) to beta carbon (Cβ) on (*S*)-epoxide ring, $r_S = \alpha_S/\beta_S = 7.3$), compared with that toward the (*R*)-enantiomer ($r_R = \beta_R/\alpha_R = 49.0$).[7a,e] Therefore, the enzyme regioselectivity toward the (*S*)-epoxide requires improvements to overcome the deficiency in *Vr*EH2-catalyzed enantioconvergent hydrolysis. Despite efforts toward enhancing the enantioconvergence of some epoxide hydrolases through directed evolution,[8] precise control of the enzyme regioselectivity to achieve perfect enantioconvergence (>99% yield, > 99% *ee*) remains challenging in EH biocatalysis.

In recent years, structure based reshaping the binding pocket or redesigning the active site has been employed to modulate the catalytic properties of enzymes, including their activity and regio/enantioselectivity.[9] Furthermore, crystallographic and computational studies have been conducted to explore the enantioconvergent behavior of EHs using molecular dynamics simulations and quantum mechanical calculations.[10] However, little progress has been made to obtain perfect enantioconvergence of epoxide hydrolases.

To rationally improve the regioselectivity of *Vr*EH2 toward (*S*)-epoxide substrates, the structure of *Vr*EH2 was determined by molecular replacement and refined to a resolution of 2.5 Å (Table S2). The *Vr*EH2 structure belongs to a typical α/β-hydrolase fold and has a particularly hydrophobic binding pocket.[11] The pocket entrance is surrounded by two oxyanion hole residues (Tyr150 and Tyr232) and a nucleophilic residue (Asp101), while the interior cavity of the pocket is mainly composed of a catalytic residue (His297) and four hydrophobic residues (Phe33, Ile176, Phe196, and Met263; Figure 1). We

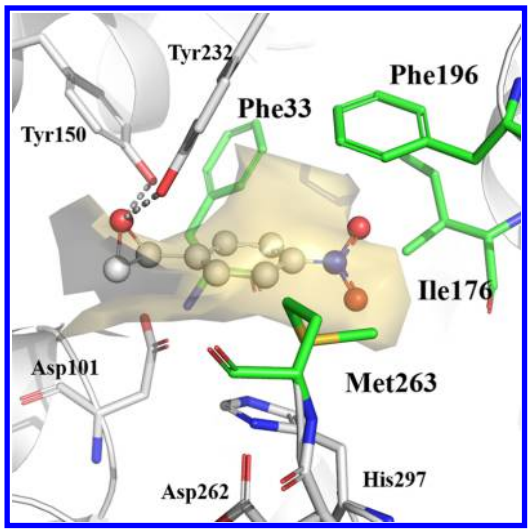

Figure 1. Structural insight of key residues lining the substrate binding pocket. The substrate (*S*)-pNSO (balls and sticks) was docked into active center, where the epoxide ring of (*S*)-pNSO is close to the oxyanion hole residues Tyr150 and Tyr232, and the nucleophilic residue Asp101, whereas the nitro group of (*S*)-pNSO is oriented toward the inside cavity of binding pocket. The gray dash: the hydrogen-bonds interaction between the oxyanion hole residues and epoxide ring of (*S*)-pNSO. The putatively sensitive residues are highlighted in green color by analyzing the interactions between (*S*)-pNSO and protein with AutoDock Tools. The catalytic residues (gray) are shown in sticks, and the binding pocket (as shown in gold shadow) was calculated by POVME.

selected four potentially candidate residues (Phe33, Ile176, Phe196, and Met263) that lined the binding site of *Vr*EH2 for engineering the regioselectivity toward (*S*)-pNSO. For reducing the screening effort, a "reduced amino acid alphabet" was employed to construct a smart library of mutants.[9b−c] The small alphabet tends to consist of amino acids with hydrophobic and hindered side chain, thus can easily reshape the binding pocket and find the key residues for further fine-tuning.[9b,d] Herein, each of the four residues was replaced with a set of amino acids (Val, Asn, Phe, and Trp), with consideration given to polarity and side-chain size effects.

Herein, we define the regioselectivity as the ratio (r) of the enzyme attacking frequencies at Cα and Cβ, which were measured experimentally using the molar ratio of diol isomers obtained using optically pure (*S*)- or (*R*)-epoxides as substrates. As shown in Figure 2, mutagenesis at residue Met263

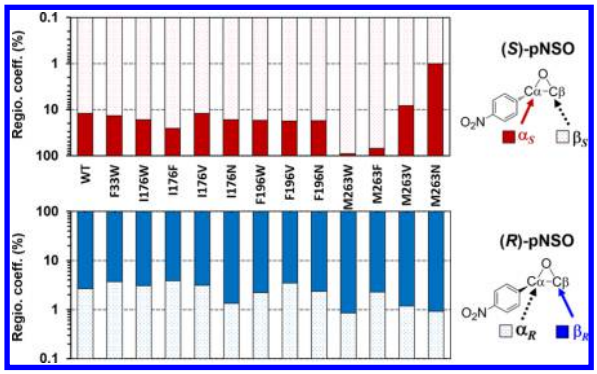

Figure 2. Measured regioselectivity of *Vr*EH2 and mutants toward (*S*)-pNSO and (*R*)-pNSO. α_S and β_S are regioselectivity coefficients which indicate the attacking percentage of Cα and Cβ of (*S*)-epoxides, respectively.

significantly affected the regioselectivity toward (*S*)-pNSO. When Met263 was mutated to Val, a residue with smaller side-chain, the specificity for Cα was improved. In contrary, when Met263 was mutated to sterically hindered residues (Phe or Trp), the regiospecificity for Cα dramatically decreased. In mutant M263N, the r_S value was increased 13.6-fold, reaching up to 99.0 (Table S3), which represented the highest regioselectivity among the tested mutants. These results demonstrated that the regioselectivity could be regulated efficiently through a single mutation of Met263 (Figure 2). We also found that mutant M263N retained its original excellent regioselectivity toward (*R*)-pNSO (r_R = 99.0) (Table S4), enabling a near-perfect enantioconvergent reaction. The regioselectivities of all mutants other than Met263 decreased to various extents, indicating that these residues (Phe33, Ile176, and Phe196) played vital role in maintaining the initial regioselectivity.

To verify the improved enantioconvergence obtained using *Vr*EH2$_{M263N}$, we performed a 10 mL scale reaction using 100 mM *rac*-pNSO and 15 g/L of the lyophilized cell free extract of *Vr*EH2$_{M263N}$. The reaction was completed within 3 h, affording final product (*R*)-pNPG with 98% *ee* and 92% isolated yield. These results confirmed the outstanding performance of the engineered enzyme in the enantioconvergent hydrolysis of racemic epoxides. To our knowledge, *Vr*EH2$_{M263N}$ is so far the best choice of biocatalyst with the highest enantioconvergence for *rac*-pNSO among all EHs reported. Furthermore, the general effect of the redesigned residue on tuning enantioconvergence

DOI: 10.1021/acscatal.8b02622
ACS Catal. 2018, 8, 8314−8317

among EHs was also examined (Table S7). The results showed that the predicted hot spot also played an essential role in regulating the activity and regioselectivity of the homologous epoxide hydrolases possessing over 58% identities to *Vr*EH2. We also determined the enantioconvergence of WT and mutant M263N toward racemic styrene oxide and racemic *meta*-nitrostyrene oxide. Compared with WT, M263N also showed improved enantioconvergence toward the other two substrates (Table S8), indicating that site 263 is very crucial for the regioselectivity regulation.

The structure of the *Vr*EH2$_{M263N}$ complex with (*S*)-pNSO contained two hydrogen bonds formed between the side chain of Asn263 and the nitro group of the substrate in *Vr*EH2$_{M263N}$ (Figure 3b) that were not observed in the docking results of

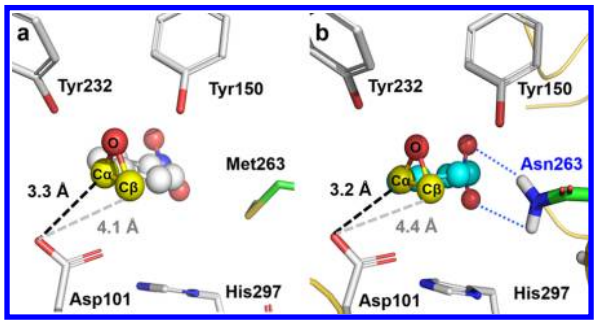

Figure 3. Substrate binding conformations of *Vr*EH2 (a, docking result) and *Vr*EH2$_{M263N}$ (b, complex). The distance between the two carbon atoms (Cα and Cβ) of epoxide ring and the nucleophile residue Asp101 is highlighted. Balls and sticks: (*S*)-pNSO. Black dash: $d_{C\alpha}$ (distance between Cα of epoxide ring and the O$^-$ of Asp101). Gray dash: $d_{C\beta}$ (distance between Cβ of epoxide ring and the O$^-$ of Asp101). Blue dash: Hydrogen-bonding interactions between Asn263 and the nitro group of (*S*)-pNSO.

*Vr*EH2 (Figure 3a). This change greatly affected the (*S*)-pNSO binding pose, the nitro group of (*S*)-pNSO in *Vr*EH2 was shifted by 0.9 Å and deflected by as much as 36.7° toward Asn263 (Figure S3a). Furthermore, the distances between catalytic residue Asp101 and the Cα or Cβ of the epoxide ring also showed expected changes (Figure 3a and 3b). The calculated (*S*)-pNSO binding energy in mutant *Vr*EH2$_{M263N}$ (−5.00 kcal/mol) was lower than that of native *Vr*EH2 (−3.68 kcal/mol) (Table S6), which indicated that the (*S*)-pNSO bound more strongly with *Vr*EH2$_{M263N}$. Notably, the difference between the Asp101 attacking distances to the two attacked epoxide carbon atoms in *Vr*EH2$_{M263N}$ ($d_{C\alpha}^2/d_{C\beta}^2 = 0.53$) was more pronounced than that in *Vr*EH2 ($d_{C\alpha}^2/d_{C\beta}^2 = 0.64$), and the measured geometrical angles of O−Cα−O$^-$ were just within the suitable scope of attack angles for S_N2 reactions (Table S6).[12] Therefore, *Vr*EH2$_{M263N}$ was more favorable than the native *Vr*EH2 for stabilizing the (*S*)-pNSO and attacking the Cα of the (*S*)-epoxide ring exclusively.

In summary, we achieved the near-perfect enantioconvergence of *Vr*EH2 through structure-guided regioselectivity engineering. Analysis of the substrate binding conformations showed that the regioselectivity improvement in *Vr*EH2 was due to the increased difference in attacking distances to the two carbons of the epoxide ring. Our strategy to engineer the enantioconvergence of epoxide hydrolase provides an ideal solution to the critical long-term challenge in enzymatic synthesis of chiral diols.

■ ASSOCIATED CONTENT

Supporting Information

The Supporting Information is available free of charge on the ACS Publications website at DOI: 10.1021/acscatal.8b02622.

General remarks, experimental procedures, supporting section, X-ray data, HPLC analytic method, supporting figures and tables, and ^{1}H, ^{13}C NMR spectra (PDF)

■ AUTHOR INFORMATION

Corresponding Authors

*E-mail: jianhexu@ecust.edu.cn.
*E-mail: huileiyu@ecust.edu.cn.
*E-mail: jiahai@sioc.ac.cn.

ORCID

Fu-Long Li: 0000-0002-2460-3266

Author Contributions

#F.-L.L. and X.-D.K. contributed equally to this work.

Notes

The authors declare no competing financial interest.

■ ACKNOWLEDGMENTS

This work was financially supported by the National Natural Science Foundation of China (Nos. 21536004, 21672063, 31770772), Shanghai Commission of Science and Technology (No. 15JC1400403), the Strategic Priority Research Program (B) of the CAS (XDB20000000), the Fundamental Research Funds for the Central Universities (No. 22221818014) and an Open Fund of the State Key Laboratory of Bioorganic and Natural Product Chemistry, Shanghai Institute of Organic Chemistry, Chinese Academy of Sciences. We are very grateful for the access to beamline BL17U1 and BL19U1 at Shanghai Synchrotron Radiation Facility and thank the beamline staff for technical help. We thank Simon Partridge, PhD, from Liwen Bianji, Edanz Editing China, for editing the English text of a draft of this manuscript.

■ REFERENCES

(1) (a) Archelas, A.; Furstoss, R. Synthetic Applications of Epoxide Hydrolases. *Curr. Opin. Chem. Biol.* **2001**, *5*, 112−119. (b) Kotik, M.; Archelas, A.; Wohlgemuth, R. Epoxide Hydrolases and their Application in Organic Synthesis. *Curr. Org. Chem.* **2012**, *16*, 451−482.

(2) (a) Lohray, B. B. Cyclic Sulfites and Cyclic Sulfates: Epoxide like Synthons. *Synthesis* **1991**, *11*, 1035−1052. (b) Pedragosa-Moreau, S.; Morisseau, C.; Zylber, J.; Archelas, A.; Baratti, J.; Furstoss, R. Microbiological Transformations. 33. Fungal Epoxide Hydrolases Applied to the Synthesis of Enantiopure *Para*-Substituted Styrene Oxides. A Mechanistic Approach. *J. Org. Chem.* **1996**, *61*, 7402−7407. (c) Archelas, A.; Furstoss, R. Synthesis of Enantiopure Epoxides through Biocatalytic Approaches. *Annu. Rev. Microbiol.* **1997**, *51*, 491−525. (d) Kasai, N.; Suzuki, T.; Furukawa, Y. Chiral C3 Epoxides and Halohydrins: their Preparation and Synthetic Application. *J. Mol. Catal. B: Enzym.* **1998**, *4*, 237−252.

(3) (a) Rui, L. Y.; Cao, L.; Chen, W.; Reardon, K. F.; Wood, T. K. Protein Engineering of Epoxide Hydrolase from *Agrobacterium radiobacter* AD1 for Enhanced Activity and Enantioselective Production of (*R*)-1-phenylethane-1,2-diol. *Appl. Environ. Microbol.* **2005**, *71*, 3995−4003. (b) Liu, Z. Y.; Michel, J.; Wang, Z. S.; Witholt, B.; Li, Z. Enantioselective Hydrolysis of Styrene Oxide with the Epoxide Hydrolase of *Sphingomonas* sp HXN-200. *Tetrahedron: Asymmetry* **2006**, *17*, 47−52. (c) Doumeche, B.; Archelas, A.; Furstoss, R. Enzymatic Transformations 62. Preparative Scale Synthesis of Enantiopure Glycidyl Acetals Using an *Aspergillus niger* Epoxide

DOI: 10.1021/acscatal.8b02622
ACS Catal. 2018, 8, 8314−8317

Hydrolase-catalysed Kinetic Resolution. *Adv. Synth. Catal.* **2006**, *348*, 1948−1957.
(4) (a) Bellucci, G.; Chiappe, C.; Cordoni, A. Enantioconvergent Transformation of Racemic *cis*-*β*-alkyl Substituted Styrene Oxides to (*R*,*R*) Threo Diols by Microsomal Epoxide Hydrolase Catalyzed Hydrolysis. *Tetrahedron: Asymmetry* **1996**, *7*, 197−202. (b) Kroutil, W.; Mischitz, M.; Plachota, P.; Faber, K. Deracemization of (±)-*cis*-2,3-epoxyheptane via Enantioconvergent Biocatalytic Hydrolysis Using *Nocardia* EH1-Epoxide Hydrolase. *Tetrahedron Lett.* **1996**, *37*, 8379−8382. (c) Orru, R. V. A.; Archelas, A.; Furstoss, R.; Faber, K. Epoxide Hydrolases and their Synthetic Applications. *Adv. Biochem. Eng./Biotechnol.* **1999**, *63*, 145−167. (d) Steinreiber, A.; Faber, K. Microbial Epoxide Hydrolases for Preparative Biotransformations. *Curr. Opin. Biotechnol.* **2001**, *12*, 552−558. (e) Steinreiber, A.; Mayer, S. F.; Saf, R.; Faber, K. Biocatalytic Asymmetric and Enantioconvergent Hydrolysis of Trisubstituted Oxiranes. *Tetrahedron: Asymmetry* **2001**, *12*, 1519−1528.
(5) (a) Mischitz, M.; Mirtl, C.; Saf, R.; Faber, K. Regioselectivity of *Rhodococcus* NCIMB 11216 Epoxide Hydrolase: Applicability of *E*-values for Description of Enantioselectivity Depends on Substrate Structure. *Tetrahedron: Asymmetry* **1996**, *7*, 2041−2046. (b) Moussou, P.; Archelas, A.; Baratti, J.; Furstoss, R. Microbiological Transformations. Part 39: Determination of the Regioselectivity Occurring During Oxirane Ring Opening by Epoxide Hydrolases: a Theoretical Analysis and a New Method for its Determination. *Tetrahedron: Asymmetry* **1998**, *9*, 1539−1547. (c) Lee, E. Y. Epoxide Hydrolase-mediated Enantioconvergent Bioconversions to Prepare Chiral Epoxides and Alcohols. *Biotechnol. Lett.* **2008**, *30*, 1509−1514.
(6) (a) Orru, R. V. A.; Kroutil, W.; Faber, K. Deracemization of (+)-2,2-disubstituted Epoxides via Enantioconvergent Chemoenzymic Hydrolysis Using *Nocardia* EH1 Epoxide Hydrolase and Sulfuric Acid. *Tetrahedron Lett.* **1997**, *38*, 1753−1754. (b) Monterde, M. I.; Lombard, M.; Archelas, A.; Cronin, A.; Arand, M.; Furstoss, R. Enzymatic Transformations. Part 58: Enantioconvergent Biohydrolysis of Styrene Oxide Derivatives Catalysed by the *Solanum tuberosum* Epoxide Hydrolase. *Tetrahedron: Asymmetry* **2004**, *15*, 2801−2805.
(7) (a) Xu, W.; Xu, J. H.; Pan, J.; Gu, Q.; Wu, X. Y. Enantioconvergent Hydrolysis of Styrene Epoxides by newly Discovered Epoxide Hydrolases in *mung bean*. *Org. Lett.* **2006**, *8*, 1737−1740. (b) Hwang, S.; Choi, C. Y.; Lee, E. Y. Enantioconvergent Bioconversion of *p*-chlorostyrene Oxide to (*R*)-*p*-chlorophenyl-1,2-ethandiol by the Bacterial Epoxide Hydrolase of *Caulobacter crescentus*. *Biotechnol. Lett.* **2008**, *30*, 1219−1225. (c) Kotik, M.; Štěpánek, V.; Grulich, M.; Kyslík, P.; Archelas, A. Access to Enantiopure Aromatic Epoxides and Diols Using Epoxide Hydrolases Derived from Total Biofilter DNA. *J. Mol. Catal. B: Enzym.* **2010**, *65*, 41−48. (d) Zhu, Q. Q.; He, W. H.; Kong, X. D.; Fan, L. Q.; Zhao, J.; Li, S. X.; Xu, J. H. Heterologous Overexpression of *Vigna radiata* Epoxide Hydrolase in *Escherichia coli* and its Catalytic Performance in Enantioconvergent Hydrolysis of *p*-nitrostyrene Oxide into (*R*)-*p*-nitrophenyl Glycol. *Appl. Microbiol. Biotechnol.* **2014**, *98*, 207−18. (e) Wu, Y. W.; Kong, X. D.; Zhu, Q. Q.; Fan, L. Q.; Xu, J. H. Chemoenzymatic Enantioconvergent Hydrolysis of *p*-nitrostyrene Oxide into (*R*)-*p*-nitrophenyl Glycol by a Newly Cloned Epoxide Hydrolase *Vr*EH2 from *Vigna radiata*. *Catal. Commun.* **2015**, *58*, 16−20. (f) Ye, H. H.; Hu, D.; Shi, X. L.; Wu, M. C.; Deng, C.; Li, J. F. Directed Modification of a Novel Epoxide Hydrolase from *Phaseolus vulgaris* to Improve its Enantioconvergence towards Styrene Epoxides. *Catal. Commun.* **2016**, *87*, 32−35.
(8) (a) Zheng, H.; Kahakeaw, D.; Acevedo, J. P.; Reetz, M. T. Directed Evolution of Enantioconvergency: the Case of an Epoxide Hydrolase-Catalyzed Reaction of a Racemic Epoxide. *ChemCatChem* **2010**, *2*, 958−961. (b) Kotik, M.; Archelas, A.; Famerova, V.; Oubrechtova, P.; Kren, V. Laboratory Evolution of an Epoxide Hydrolase - towards an Enantioconvergent Biocatalyst. *J. Biotechnol.* **2011**, *156*, 1−10. (c) Kotik, M.; Zhao, W.; Iacazio, G.; Archelas, A. Directed Evolution of Metagenome-derived Epoxide Hydrolase for Improved Enantioselectivity and Enantioconvergence. *J. Mol. Catal. B: Enzym.* **2013**, *91*, 44−51.
(9) (a) Wu, Q.; Soni, P.; Reetz, M. T. Laboratory Evolution of Enantiocomplementary *Candida antarctica* Lipase B Mutants with Broad Substrate Scope. *J. Am. Chem. Soc.* **2013**, *135*, 1872−1881. (b) Kong, X. D.; Ma, Q.; Zhou, J.; Zeng, B. B.; Xu, J. H. A Smart Library of Epoxide Hydrolase Variants and the Top Hits for Synthesis of (*S*)-*β*-Blocker Precursors. *Angew. Chem., Int. Ed.* **2014**, *53*, 6641−6644. (c) Sun, Z.; Lonsdale, R.; Kong, X. D.; Xu, J. H.; Zhou, J.; Reetz, M. T. Reshaping an Enzyme Binding Pocket for Enhanced and Inverted Stereoselectivity: Use of Smallest Amino Acid Alphabets in Directed Evolution. *Angew. Chem., Int. Ed.* **2015**, *54*, 12410−12415. (d) Sun, Z.; Lonsdale, R.; Wu, L.; Li, G.; Li, A.; Wang, J.; Zhou, J.; Reetz, M. T. Structure-Guided Triple-Code Saturation Mutagenesis: Efficient Tuning of the Stereoselectivity of an Epoxide Hydrolase. *ACS Catal.* **2016**, *6*, 1590−1597. (e) Balke, K.; Schmidt, S.; Genz, M.; Bornscheuer, U. T. Switching the Regioselectivity of a Cyclohexanone Monooxygenase toward (+)-*trans*-Dihydrocarvone by Rational Protein Design. *ACS Chem. Biol.* **2016**, *11*, 38−43. (f) Sun, Z.; Salas, P. T.; Siirola, E.; Lonsdale, R.; Reetz, M. T. Exploring Productive Sequence Space in Directed Evolution Using Binary Patterning versus Conventional Mutagenesis Strategies. *Bioresour. Bioprocess.* **2016**, *3*, 44. (g) Chen, X.; Zhang, H.; Feng, J.; Wu, Q.; Zhu, D. Molecular Basis for the High Activity and Enantioselectivity of the Carbonyl Reductase from *Sporobolomyces salmonicolor* toward *α*-Haloacetophenones. *ACS Catal.* **2018**, *8*, 3525−3531.
(10) (a) Amrein, B. A.; Bauer, P.; Duarte, F.; Janfalk Carlsson, A.; Naworyta, A.; Mowbray, S. L.; Widersten, M.; Kamerlin, S. C. L. Expanding the Catalytic Triad in Epoxide Hydrolases and Related Enzymes. *ACS Catal.* **2015**, *5*, 5702−5713. (b) Bauer, P.; Carlsson, A. J.; Amrein, B. A.; Dobritzsch, D.; Widersten, M.; Kamerlin, S. C. L. Conformational Diversity and Enantioconvergence in Potato Epoxide Hydrolase 1. *Org. Biomol. Chem.* **2016**, *14*, 5639−5651. (c) Lind, M. E. S.; Himo, F. Quantum Chemical Modeling of Enantioconvergency in Soluble Epoxide Hydrolase. *ACS Catal.* **2016**, *6*, 8145−8155.
(11) (a) Durrant, J. D.; de Oliveira, C. A. F.; McCammon, J. A. POVME: an Algorithm for Measuring Binding-pocket Volumes. *J. Mol. Graphics Modell.* **2011**, *29*, 773−776. (b) Durrant, J. D.; Votapka, L.; Sørensen, J.; Amaro, R. E. POVME 2.0: An Enhanced Tool for Determining Pocket Shape and Volume Characteristics. *J. Chem. Theory Comput.* **2014**, *10*, 5047−5056.
(12) (a) Lacourciere, G. M.; Armstrong, R. N. The Catalytic Mechanism of Microsomal Epoxide Hydrolase Involves an Ester Intermediate. *J. Am. Chem. Soc.* **1993**, *115*, 10466−10467. (b) Borhan, B.; Jones, A. D.; Pinot, F.; Grant, D. F.; Kurth, M. J.; Hammock, B. D. Mechanism of Soluble Epoxide Hydrolase. Formation of an Alpha-hydroxy Ester-enzyme Intermediate through Asp-333. *J. Biol. Chem.* **1995**, *270*, 26923−26930. (c) Schiott, B.; Bruice, T. C. Reaction Mechanism of Soluble Epoxide Hydrolase: Insights from Molecular Dynamics Simulations. *J. Am. Chem. Soc.* **2002**, *124*, 14558−14570. (d) Hopmann, K. H.; Himo, F. Insights into the Reaction Mechanism of Soluble Epoxide Hydrolase from Theoretical Active Site Mutants. *J. Phys. Chem. B* **2006**, *110*, 21299−21310. (e) Jochens, H.; Stiba, K.; Savile, C.; Fujii, R.; Yu, J. G.; Gerassenkov, T.; Kazlauskas, R. J.; Bornscheuer, U. T. Converting an Esterase into an Epoxide Hydrolase. *Angew. Chem., Int. Ed.* **2009**, *48*, 3532−3535. (f) Sun, Z.; Wu, L.; Bocola, M.; Chan, H. C. S.; Lonsdale, R.; Kong, X. D.; Yuan, S.; Zhou, J.; Reetz, M. T. Structural and Computational Insight into the Catalytic Mechanism of Limonene Epoxide Hydrolase Mutants in Stereoselective Transformations. *J. Am. Chem. Soc.* **2018**, *140*, 310−318.

NOTE ADDED AFTER ASAP PUBLICATION

This paper published ASAP on August 13, 2018 with a misspelling in author Guo-Qiang Lin's name. The corrected paper reposted to the Web on August 17, 2018.

DOI: 10.1021/acscatal.8b02622
ACS Catal. 2018, 8, 8314−8317